

A novel bis-phenanthridine triamine with pH controlled binding to nucleotides and nucleic acids

Goran Malojčić,^{†a} Ivo Piantanida,^{*a} Mirna Marinić,^a Mladen Žinić,^a Marko Marjanović,^b Marijeta Kralj,^b Krešimir Pavelić^b and Hans-Jörg Schneider^c

^a Laboratory for Supramolecular and Nucleoside Chemistry Ruđer Bošković Institute, P.O.B. 180, HR-10002, Zagreb, Croatia. E-mail: pianta@irb.hr; Fax: +385 1 46 80 195; Tel: +385 1 45 71 210

^b Laboratory of Functional Genomics, Division of Molecular Medicine, Ruđer Bošković Institute, P.O. Box 180, HR-10002, Zagreb, Croatia. E-mail: mhorvat@irb.hr; Fax: +385 1 45 61 010; Tel: +385 1 45 71 235

^c FR Organische Chemie der Universität des Saarlandes, D 66041, Saarbrücken, Germany. E-mail: ch12hs@rz.uni-sb.de; Fax: +49 (0)681 302 4105; Tel: +49 (0)681 302 3209/2269

Received 28th June 2005, Accepted 14th October 2005

First published as an Advance Article on the web 10th November 2005

The new bis-phenanthridine triamine (**3**) is characterised by three pK_a values: 3.65; 6.0 and >7.5. A significant difference in the protonation state of **3** at pH = 5 (four positive charges) and at pH = 7 (less than two positive charges) accounts for the strong dependence of **3**-nucleotide binding constants on nucleotide charge under acidic conditions, whereas at neutral pH all **3**-nucleotide complexes are of comparable stability. All experimental data point at intercalation as the dominant binding mode of **3** to polynucleotides. However, there is no indication of bis-intercalation of the two phenanthridine subunits in binding to double stranded polynucleotides, the respective complexes being most likely mono-intercalative. Thermal stabilisation of calf thymus DNA (ct-DNA) and poly A-poly U duplexes upon addition of **3** is significantly higher at pH = 5 than at neutral conditions. This is not the case with poly dA-poly dT, indicating that the specific secondary structure of the latter, most likely the shape of the minor groove, plays a key role in complex stability. At pH = 5 **3** acts as a fluorimetric probe for poly G (emission quenching) as opposed to other ss-polynucleotides (emission increase), while at neutral conditions this specificity is lost. One order of magnitude higher cytotoxicity of **3** compared to its "monomer" **4** can be accounted for by cooperative action of two phenanthridinium units and the charged triamine linker. The results presented here are of interest to the development of *e.g.* sequence-selective cytostatic drugs, and in particular for the possibility to control the drug activity properties over binding to DNA and/or RNA by variation of the pH of its surrounding.

Introduction

Numerous drugs base their biological activity on interaction of low molecular weight organic molecules with DNA and/or RNA. Therefore design, synthesis, and biological evaluation of novel compounds that target these macromolecules and whose interactions could lead to a better understanding of recognition processes are of high interest. Small molecules of this kind are of special interest because they can more easily cross biological membranes than large molecules, and can even be delivered to cells strongly resistant to exogenous matter. *E.g.* brain cells resist the entry of molecules with MW larger than approximately 600, thus disabling cancer treatment.

In general, there are three main modes of binding of small molecules to DNA/RNA, (i) minor groove binding, (ii) intercalation and (iii) pure electrostatic interaction of highly positively charged molecules with the nucleotide phosphate backbone.¹ Many authors combined more modes of interaction in the same molecule aiming at very specific goals such as increased sequence selectivity,² enhanced affinity,³ or some specific actions like cleavage.⁴ Aliphatic polyamines bearing a variety of aromatics at the terminal amino groups are a good example of two DNA/RNA binding modes combined: positively charged amines interact with the polynucleotide phosphate backbone while aromatics intercalate. Such molecules

exhibit various highly interesting properties, and are used as fluorescent chemosensors,⁵ selective receptors for nucleotides, nucleosides and single-stranded sequences in DNA,⁶ highly efficient DNA/RNA bis-intercalators³ as well as light-driven pH-regulated molecular machines.⁷ Especially the latter property has led us to perform a more detailed investigation on the possible use of such compounds as pH-controlled binders to DNA or RNA.

In order to be able to assess which role individual structural features of such molecules play in interactions with its biological targets, we have decided to work in a simple and well-defined system. Diethylenetriamine was chosen as linker since its length (7 atoms + 2 carbons of the aromatic system attached) theoretically allows bis-intercalation of terminally attached aromatics.³ We decided to use unsubstituted phenanthridine as the aromatic moiety for the following reasons: (i) the pK_a value of the heteroaromatic nitrogen is about 6, thus at pH = 5 and 7 the novel molecule consisting of the triamine linker and two phenanthridines would bear significantly different numbers of positive charges and therefore be ideal for comparison of neutral and weakly acidic conditions (both of biological relevance), (ii) the compound should bind to DNA/RNA by intercalation since the phenanthridine derivatives are well-known intercalators and (iii) the phenanthridine moiety, characterised by high fluorescence emission, offers not only use of this sensitive method for analytical purposes, but also possible application of the molecule as a fluorescent marker analogous to bis-methidium spermine.⁸ It should be stressed that our novel molecule differs essentially from its above mentioned methidium spermine analogue, the latter being methylated at the phenanthridine heteroaromatic

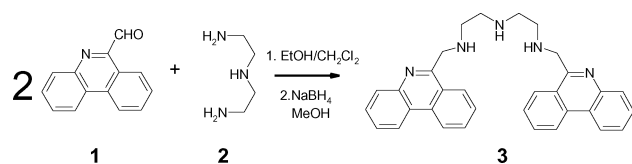
[†] Present address: Institut für Molekularbiologie und Biophysik, Eidgenössische Technische Hochschule Hönggerberg (ETH Zürich), CH-8093 Zürich, Switzerland. Fax: +41 44 633 1036; Tel: +41 44 6332482; E-mail: goran@mol.biol.ethz.ch

nitrogen, thus unavailable for protonation and insensitive to pH values. It is worth stressing that compounds with significantly increased protonation rate at weakly acidic conditions ($pK_a \approx 6$) hold some promise as targets for different acidic solid tumor tissues.⁹

Results and discussion

Synthesis

Coupling starting compounds **1** and **2** by a simple synthetic procedure as shown in Scheme 1 (for details see Experimental) gave compound **3** in a good yield. Although the same procedure worked well in previously reported syntheses of various diaryl-polyamines,⁶ some details in the preparation of **3** require more attention. In the preparation of phenanthridine-5-aldehyde (**1**) from the 5-methyl precursor,¹⁰ SeO_2 should be used in smallest possible excess (<5%), otherwise inorganic by-products are extremely difficult to remove, partially hamper the reactions presented in Scheme 1, and disable efficient purification of the final product **3** by successive re-crystallizations.



Scheme 1 Synthesis of **3**.

Spectroscopy

Compound **3** is readily soluble in water up to the concentration of $5 \times 10^{-3} \text{ mol dm}^{-3}$. An aqueous solution of **3** is characterised by a UV/Vis spectrum with absorbance maxima at $\lambda_{\text{max}} = 244, 332$ and 348 nm . An aqueous solution of **3** exhibits strong fluorescence with emission maximum at $\lambda_{\text{max}} = 400 \text{ nm}$; excitation spectrum being in good accordance with the UV/Vis spectrum. The UV/Vis and in particular fluorescence emission spectra of aqueous solutions of **3** are pH dependent, with three main transition steps characterised by $pK_a = 3.6; 6.0$ and >7.5 , respectively. According to the literature data, the first transition step (most pronounced in fluorescence changes of **3**) can be attributed to the protonation equilibrium of the central amino group of the aliphatic linker,⁷ whereas the second transition step (less pronounced in fluorescence changes of **3**) characterizes protonation of the two equivalent phenanthridine nitrogens.¹¹ The third transition could be only estimated due to partial precipitation of **3**, but it most likely comprises two protonations of the remaining amines in the linker ($pK_a = 7.81$ and $pK_a = 8.38$, as reported for a close analogue of **3**).⁷ It is well known that the number of positive charges in the small molecule profoundly influences its interactions with polynucleotides. Therefore, we have chosen to perform comparative studies on binding of **3** to DNA/RNA at pH = 5 (**3** characterised by four positive charges, two phenanthridinium units protonated) and at pH = 7, at which **3** bears less than two positive charges (aliphatic amines $pK_a > 7.5$),⁷ with two phenanthridinium units not protonated and thus neutral.

The UV/Vis and fluorescence spectra of **3** at both pH = 5 and pH = 7 obey the Lambert–Beer law in the concentration range of $5 \times 10^{-6} - 8 \times 10^{-5} \text{ mol dm}^{-3}$ and $5 \times 10^{-7} - 1 \times 10^{-5} \text{ mol dm}^{-3}$, respectively. Molar extinction coefficients of **3** at used pH's differ by about 7% due to different protonation of **3** (Table 1).

Temperature dependent changes of the UV/Vis spectra in the range between $25 \text{ }^\circ\text{C}$ and $90 \text{ }^\circ\text{C}$ resulted in less than 5% hypochromicity at both pH = 5 and pH = 7, which indicates that intramolecular stacking interactions between the phenanthridine units of **3** are very weak or not existing. Although the combined influence of strong hydrophobic effects

Table 1 Molar extinction coefficients of **3** at pH = 5 and pH = 7 (sodium cacodylate buffer, $I = 0.05 \text{ mol dm}^{-3}$)

pH	λ/nm	$\epsilon/\text{mol}^{-1} \text{ cm}^2$
5.0	244	63827
	332	2718
	348	2358
7.0	244	59115
	332	4429
	348	3840

and aromatic $\pi \cdots \pi$ stacking interactions favors intermolecular aggregation of large aromatic systems in aqueous media, linear dependence of absorbance on concentration of **3** excludes this possibility. Most probably, repulsion of positive charges located at the terminal amines of the linker hinders intramolecular aggregation of the tethered phenanthridine units.

Aqueous solutions of **3** were stable for three days, after which a substantial decrease and systematic changes in the UV/Vis spectrum were observed, attributed to the chemical degradation of **3**. Therefore, all experiments were performed with fresh solutions.

Interactions of **3** with nucleotides

Addition of nucleotides to aqueous solutions of **3** at both pH = 5 and 7 induced minor changes in the UV/Vis spectrum of **3**, but significant quenching of **3** fluorescence emission. An excitation wavelength of **3** at $\lambda_{\text{max}} = 332 \text{ nm}$ was used for fluorimetric titrations since nucleotides do not absorb light at $\lambda > 300 \text{ nm}$ and at $\lambda > 340 \text{ nm}$ excitation and emission spectra of **3** significantly overlap. To obtain the binding constants (K_s), fluorescence titration data were processed by SPECFIT¹² giving in most cases the best fit for the **3**–nucleotide (nucleoside) complexes of 1 : 1 and 1 : 2 stoichiometries. Experimental data in the range of 20–80% of complex formation could be collected for only 1 : 1 stoichiometry, while formation of 1 : 2 stoichiometry complexes for most titration experiments were observed in less than 20%; therefore binding constants for the latter stoichiometry can be considered only as an estimate. In general, binding constants for 1 : 1 stoichiometry found for purine nucleotides are significantly higher than those observed for pyrimidine nucleotides (Table 2 and Fig. 1), which suggests significant contribution of aromatic $\pi \cdots \pi$ stacking interactions in **3**–nucleotide complexes.¹³

Fluorimetric titrations at pH = 5 of **3** with adenosine series differing in the number of phosphates (Fig. 1a) reflect a strong impact of the number of nucleotide negative charges on the binding affinity of **3** towards it. The value of K_s

Table 2 Binding constants ($\log K_s$) for various **3**–nucleotide complexes of 1 : 1 stoichiometry obtained from fluorimetric titrations at pH = 5 and pH = 7^a

	$\log K_s$ (pH = 5)	$\log K_s$ (pH = 7)
ATP	3.54 ± 0.12	3.67 ± 0.06
ADP	2.64 ± 0.05	3.32 ± 0.03
AMP	2.29 ± 0.03	2.98 ± 0.04
Adenosine	2.10 ± 0.27^b	^b
GMP	2.20 ± 0.05	3.27 ± 0.1
CMP	2.12 ± 0.05	2.32 ± 0.18

^a For both pH's titrations were performed in sodium cacodylate buffer, $I = 0.05 \text{ mol dm}^{-3}$. Data were processed by SPECFIT,¹² in most cases yielding the best fit for 1 : 1 and 1 : 2 stoichiometry complexes; only values for the former are given for easier comparison, while the latter could be only estimated as follows: $\log K_s$ (purine bases) = 1–2; $\log K_s$ (CMP) < 1. ^b Low solubility of adenosine allowed collection of titration data only up to 50% of complex formation at pH = 5, thus the higher error of the respective $\log K_s$ value; even lower solubility at pH = 7 made measurements impossible.

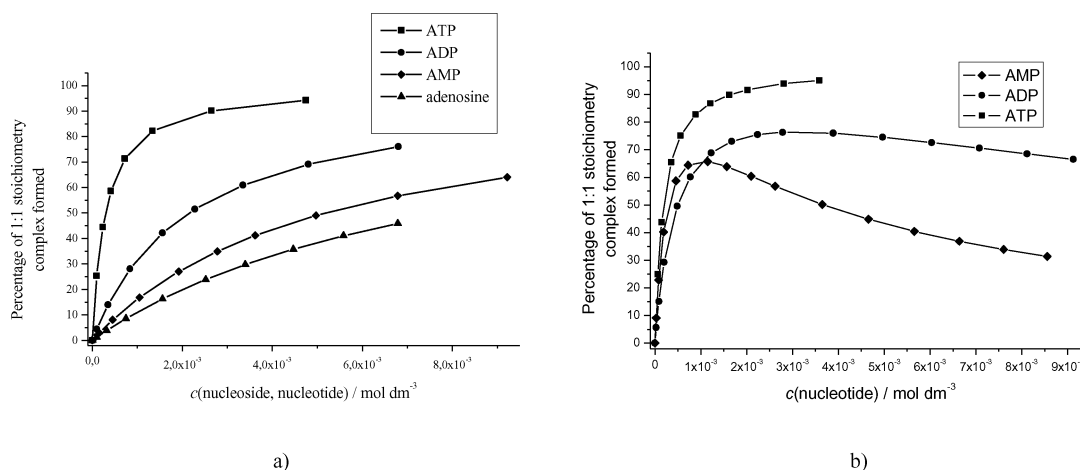


Fig. 1 Fluorimetric titrations with adenosine series differing in the number of phosphates. Dependence of calculated 1 : 1 stoichiometry complex formation on concentration of nucleotide or nucleoside added to **3** is depicted (sodium cacodylate buffer, $I = 0.05 \text{ mol dm}^{-3}$), a) at $\text{pH} = 5$, b) at $\text{pH} = 7$.

obtained for **3**-adenosine is in good accordance with affinities of other phenanthridinium analogues forming complexes with nucleotides and nucleosides based solely on aromatic $\pi \cdots \pi$ stacking interactions.¹⁴⁻¹⁶ This finding suggests that at $\text{pH} = 5$ there is no chelate effect of phenanthridine subunits of **3** in nucleoside binding. The observed substantial increase of K_s values (Table 2, $\text{pH} = 5$) reflects the increase of the number of negatively charged phosphates attached to adenosine, in agreement with electrostatic interactions between negative charges of the nucleotide phosphates and the positive charges of **3**. A possible explanation for this tendency is that aromatic stacking between nucleobase and one phenanthridinium unit of **3** has a certain constant value and every additional negatively charged phosphate substantially contributes to the cumulative affinity. This presumption is in accordance with significantly less pronounced corresponding increase in the K_s values with increasing number of adenosine phosphates at $\text{pH} = 7$ (Fig. 1b, Table 2) since at that pH compound **3** bears less than half positive charges than at $\text{pH} = 5$.

Another point to stress is the influence of pH (*i.e.* protonation state of **3**) on the binding affinity of **3** towards the same nucleotide (Table 2, Fig. 1a,b). For all nucleotides, K_s values at $\text{pH} = 7$ are higher than those at $\text{pH} = 5$. Also, affinities of the bis-phenanthridinium derivative **3** toward most of the nucleotides are almost an order of magnitude higher than those of its "monomeric" analogues bearing a single phenanthridinium moiety.¹⁴⁻¹⁶ Such increased affinities cannot be accounted for by the possible intercalation of nucleotide base between phenanthridine units of **3** because the chelate effect observed for such "sandwich type complexes", with previously studied bis-phenanthridinium analogues, resulted in more than two orders of magnitude higher K_s compared to the corresponding monomers.¹³ Therefore, the only possible reason for the increased affinity at $\text{pH} = 7$ is the difference in binding affinity of phenanthridinium (dominant at $\text{pH} = 5$) and phenanthridine (dominant at $\text{pH} = 7$) towards the aromatic moiety of nucleotides. Significantly higher hydrophobicity of phenanthridine compared to phenanthridinium should therefore be responsible for the increased affinity toward nucleotides at $\text{pH} = 7$.

Interactions with double stranded (ds-) DNA and RNA

UV/Vis titrations. The UV/Vis spectrum of **3** is characterised by strong absorption maximum at 244 nm and two much weaker maxima over 300 nm (Table 1). Due to the low solubility of **3**-polynucleotide complexes, $c(\mathbf{3}) = 2 \times 10^{-5} \text{ mol dm}^{-3}$ had to be used, where only absorption at $\lambda_{\text{max}} = 244 \text{ nm}$

was strong enough for studying interactions with DNA and RNA. At $\text{pH} = 7$ addition of any polynucleotide yielded instant precipitation. On the contrary, at $\text{pH} = 5$ **3**-polynucleotide complexes were significantly more soluble. Titration experiments were performed by collecting changes in the UV/Vis spectra of **3** in the range $\lambda = 220\text{--}300 \text{ nm}$ upon addition of polynucleotide into the buffered solution ($\text{pH} = 5$) of **3**. Addition of all studied polynucleotides at excess **3** up to the ratios $r_{a[\mathbf{3}]/[\text{polynucleotide}]}$ (Table 3) showed a decrease in UV/Vis absorption, this observation being in clear contrast with the fact that polynucleotides also absorb light in this range and therefore total absorption of the sample should increase. In all experiments isosbestic points could be observed at these conditions, indicating coexistence of only two major light-absorbing species, the free **3** and its complex with polynucleotide. Further additions of polynucleotides (increasing excess of polynucleotides over **3**) resulted in loss of isosbestic points (ratios $r < r_a$) due to more absorbing species in solution (we assume free **3**, free polynucleotide and their complex). Therefore, in order to estimate binding affinities of **3** towards various polynucleotide substrates by spectroscopic titrations, it was necessary to analyse the data (changes in complete spectra) using the multivariate nonlinear factor analysis program SPECFIT.¹² This program, however, does not use the Scatchard equation,¹⁷ so we had to fix the Scatchard ratio $n_{[\text{bound } \mathbf{3}]/[\text{polynucleotide}]} = 0.2$ as the most common value for intercalators,¹⁸ which is also in good agreement with the ratio r_a (Table 3). The calculated binding constants (K_s) and spectroscopic properties of complexes are given in Table 3.

Fluorimetric titrations. Since **3** exhibits strong fluorescence emission, it was possible to perform fluorimetric titrations with polynucleotides. Excitation of **3** at $\lambda_{\text{max}} = 332 \text{ nm}$ was used for

Table 3 Binding constants (K_s), hypochromic effect (H) and spectroscopic properties of complexes (shift of $\lambda_{\text{max}} = 244 \text{ nm}$) calculated from UV/Vis titrations of **3** with ds-polynucleotides at $\text{pH} = 5$ (buffer citric acid, $I = 0.03 \text{ mol dm}^{-3}$)^a

	^b H	^c Shift of $\lambda_{\text{max}} = 244 \text{ nm}$	^d r_a	$\log K_s$
Poly A-poly U	0.66	+8	0.11	5.0 ± 0.1
Poly G-poly C	0.93	+16	0.20	6.2 ± 0.2
ct-DNA	0.98	+6	0.18	5.8 ± 0.2

^a Titration data were processed using the program SPECFIT¹² for $n_{[\text{bound } \mathbf{3}]/[\text{polynucleotide}]} = 0.2$ as the most common value for intercalators. ^b hypochromic effect. $H = \text{Abs}(\text{complex at } \lambda_{\text{max}} = 244 \text{ nm})/\text{Abs}(\mathbf{3} \text{ at } \lambda_{\text{max}} = 244 \text{ nm})$. ^c Shift of $\lambda_{\text{max } 244 \text{ nm}} = \lambda_{\text{max } 244 \text{ nm}}(\mathbf{3}) - \lambda_{\text{max}}(\text{complex})$. ^d The lowest ratio $r_{[\mathbf{3}]/[\text{polynucleotide}]}$ at which isosbestic points are still present.

Table 4 Binding constants (K_s), ratios $n = ([\text{bound } \mathbf{3}]/[\text{polynucleotide}])$ and spectroscopic properties of complexes of $\mathbf{3}$ ($c = 5 \times 10^{-6} \text{ mol dm}^{-3}$) with ds-polynucleotides calculated from fluorimetric titrations of $\mathbf{3}$ at pH = 5 (buffer citric acid, $I = 0.03 \text{ mol dm}^{-3}$) and pH = 7 (buffer sodium cacodylate, $I = 0.05 \text{ mol dm}^{-3}$)^a

pH		n	$\log K_s$	$^b I/I_0$
5	ct-DNA	0.22	5.87	0.61
	Poly A-poly U	0.22	5.12	0.58
	Poly G-poly C	0.13	5.81	0.57
7	ct-DNA	0.13	6.65	0.39
		^c 0.09	^c 6.34	^c 0.55
	Poly A-poly U	^d 0.001	^d 6.19	^d 1.1
	Poly G-poly C	0.08	5.22	0.26

^a Titration data were processed using the Scatchard equation, accuracy of obtained $n \pm 10\text{--}30\%$, consequently $\log K_s$ values vary in the same order of magnitude. ^b Emission change; $I = I(\text{complex})/I(\mathbf{3})$. ^c Data calculated by the Scatchard equation from the first part of titration experiment with poly A-poly U in which starting fluorescence of $\mathbf{3}$ was quenched. ^d Data calculated by the Scatchard equation from the second part of titration experiment with poly A-poly U in which fluorescence of primarily formed complex $\mathbf{3}$ -poly A-poly U was enhanced by formation of secondary complex.

fluorimetric titrations because polynucleotides do not absorb light at $\lambda > 300 \text{ nm}$ and at $\lambda > 340 \text{ nm}$ excitation and emission spectra of $\mathbf{3}$ significantly overlap. Addition of ds-polynucleotides at both pH = 5 and 7 results in strong changes of $\mathbf{3}$ fluorescence. For most titrations it was possible to process spectroscopic data using Scatchard equation, results are given in Table 4.

According to the values of K_s and n calculated from titrations performed at pH = 5, compound $\mathbf{3}$ shows similar affinity towards all studied polynucleotides. The values are in good accord with those estimated from UV/Vis titrations (Table 3). Both K_s and n values suggest mono-intercalative rather than bis-intercalative binding mode, since the affinities of classical bis-intercalators are much higher than those observed, and the values of n are much lower than 0.1.^{3,19}

It is interesting to note that only titration with poly A-poly U at pH = 7 yields quenching of $\mathbf{3}$ fluorescence until ratio $r_{[\mathbf{3}]/[\text{poly A-poly U}]} = 0.02$, and further addition of poly A-poly U yields substantial fluorescence increase (Fig. 2). Such a pattern clearly indicates formation of two different $\mathbf{3}$ -poly A-poly U complexes, significantly different either in stability or in the availability of free poly A-poly U necessary for efficient binding of $\mathbf{3}$. Fluorescence titration data of both quenching and emission increases were separately processed by means of the Scatchard equation. Processing of the part of titration data where fluorescence was quenched gave values of binding constant (K_s) and ratio n (with excellent correlation coefficients, $R > 0.999$) quite similar to those obtained for ct-DNA, but significantly higher than observed for poly G-poly C. Processing of titration data where fluorescence of $\mathbf{3}$ was enhanced gave a value of binding constant ($\log K_s = 6.2$) similar to the one found for the quenching part of titration but the value of ratio n was significantly lower ($n = 0.001$). A possible explanation of the observed two different $\mathbf{3}$ -poly A-poly U complexes is the following: a) quenching of the fluorescence could be the result of the inter-strand cross-binding of $\mathbf{3}$ to two different molecules of poly A-poly U at the conditions close to the equimolar ratio of $\mathbf{3}$ and poly A-poly U (which would dictate binding of $\mathbf{3}$ approximately once per full turn of two double helices), and b) fluorescence increase at high excess of poly A-poly U over $\mathbf{3}$ could be indicating conversion of the afore mentioned complex into a mono-intercalative complex of $\mathbf{3}$ with only a single molecule of poly A-poly U. The difference in orientation and engagement of phenanthridinium units of $\mathbf{3}$ in these two complexes could easily yield different fluorescence properties and therefore observed opposite fluorescence changes.

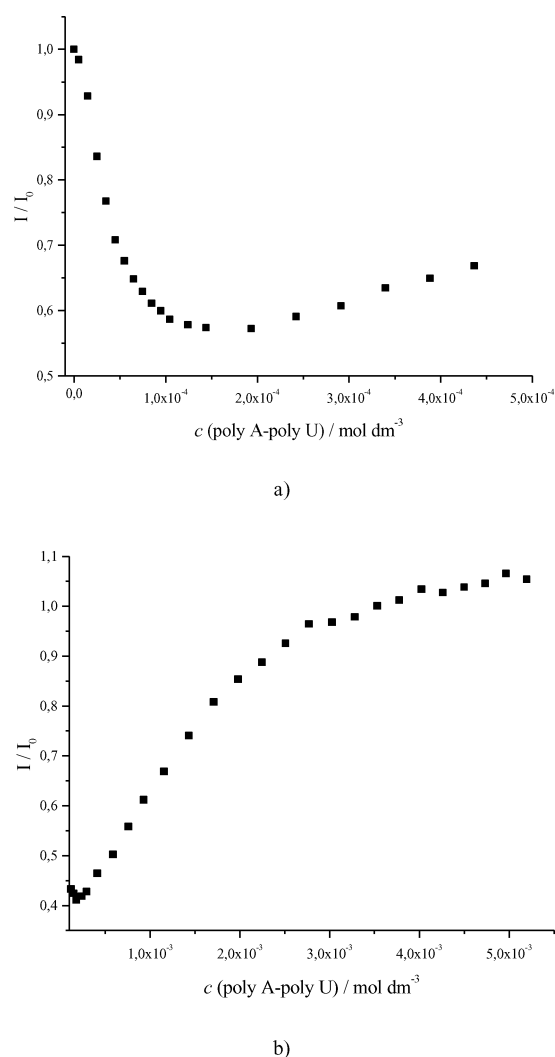


Fig. 2 Fluorimetric titration of $\mathbf{3}$ ($c = 5 \times 10^{-6} \text{ mol dm}^{-3}$) with poly A-poly U at pH = 7 (buffer sodium cacodylate, $I = 0.05 \text{ mol dm}^{-3}$), a) $r_{[\mathbf{3}]/[\text{poly A-poly U}]} = 1\text{--}0.02$; b) $r_{[\mathbf{3}]/[\text{poly A-poly U}]} = 0.02\text{--}0.0002$.

Both ds-RNA (A-U and G-C base pairs) form an A-helix at the experimental conditions (pH = 7, $I = 0.05 \text{ mol dm}^{-3}$). The poly G-poly C minor groove is sterically hindered by the amino groups of guanine, while the minor groove of poly A-poly U is not,²⁰ thus facilitating the approach of the positively charged linker of $\mathbf{3}$ to negatively charged phosphates. Therefore, if we consider that $\mathbf{3}$ is mono-intercalating into both RNA polynucleotides from the minor groove site, its positively charged linker can fit tighter to poly A-poly U, resulting in a higher binding constant than observed for poly G-poly C. The proposed tight contact of $\mathbf{3}$ into poly A-poly U minor groove at conditions of high excess of polynucleotide over $\mathbf{3}$ could result in a better accommodation of $\mathbf{3}$ and formation of other types of complex (possibly even bis-intercalative binding), with molecules of $\mathbf{3}$ covering larger areas of poly A-poly U independently of each other. This could explain the observed secondarily formed complex in fluorimetric titrations at pH = 7 (fluorescence increase) and also different binding of $\mathbf{3}$ to poly G-poly C.

At pH = 5 addition of poly A-poly U to $\mathbf{3}$ resulted only in quenching of its fluorescence. The calculated K_s value of the $\mathbf{3}$ -poly A-poly U complex was significantly lower at pH = 5 than at pH = 7 for the quenching part of the titration. At pH = 5 $\mathbf{3}$ bears double the positive charge as compared to pH = 7, but the poly A strand is partially protonated as well.²⁰ Such a high concentration of positive charges on both complex-forming species could hamper the tight fitting of $\mathbf{3}$ into the minor groove

Table 5 ΔT_m values ($^{\circ}\text{C}$) of **3** in low ionic strength buffers pH = 5.0 and pH = 7.0^{a,c}

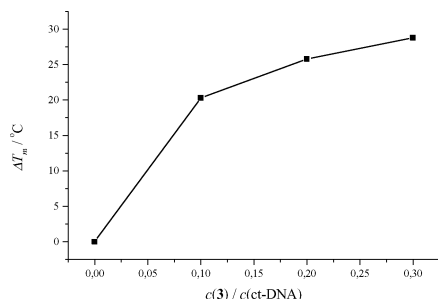
pH		$^b r$			
		0.1	0.2	0.3	0.5
5	ct-DNA	20.3	25.8	28.8	32.3
	poly A–poly U	^c 12.5	^c 9.5	^c 10.0	^d ND
	poly AH ⁺ –poly AH ⁺	^c 0	^c 0	^c 0	^c 0
	poly dA–poly dT	7.5	11.1	12.6	16.0
7	ct-DNA	4.1	5.7	6.0	7.0
	poly A–poly U	3.1	5.2	6.0	7.1
	poly dA–poly dT	8.6	12.1	14.2	15.1

^a Buffer pH = 5 (citric acid; $I = 0.03 \text{ mol dm}^{-3}$) and buffer pH = 7 (sodium cacodylate, $I = 0.05 \text{ mol dm}^{-3}$); error in ΔT_m : $\pm 0.5 \text{ }^{\circ}\text{C}$. ^b r : molar ratio of **3**/nucleic acid phosphates. ^c Biphasic transitions: the first transition at $T_m = 28.5 \text{ }^{\circ}\text{C}$ is attributed to denaturation of poly A–poly U and the second transition at $T_m = 80.1 \text{ }^{\circ}\text{C}$ is attributed to denaturation of poly AH⁺–poly AH⁺ since poly A at pH = 5 is mostly protonated and forms ds-polynucleotide.^{16,19} ^d ND: impossible to determine. ^e T_m values of free polynucleotides: pH = 5 (ct-DNA/59.2 $^{\circ}\text{C}$; polyA–polyU/28.5/81.1 $^{\circ}\text{C}$ see explanation at ^c; poly dA–poly dT/66.0 $^{\circ}\text{C}$); pH = 7 (ct-DNA/78.0 $^{\circ}\text{C}$; polyA–polyU/50.0 $^{\circ}\text{C}$; poly dA–poly dT/62.1 $^{\circ}\text{C}$).

of poly A–poly U, as it is presumed at pH = 7, and result in lower affinity at acidic pH. This explanation is consistent with a smaller difference in affinity of **3** towards poly A–poly U and poly G–poly C at pH = 5 than at pH = 7.

Thermal melting experiments. Addition of **3** to most ds-polynucleotides yielded strong thermal stabilisation of the double helices (Table 5). The only exception was poly AH⁺–poly AH⁺ monitored either as a second transition curve in poly A–poly U melting experiments or formed by protonation of a single poly A strand at pH = 5.²⁰ The reason for this is probably the high melting point of poly AH⁺–poly AH⁺ where **3** very likely does not form a stable complex. Also, repulsive forces between positively charged adenines of poly AH⁺–poly AH⁺ and four positive charges of **3** at pH = 5 could be the cause of no measurable interaction.

For all other ds-polynucleotides stabilised by **3**, an increase of the ratio r did not result in a proportional increase of ΔT_m values. According to this nonlinearity (dependence of ΔT_m values on the ratio r ; Table 5 and Fig. 3), saturation of binding sites could be estimated at about $r = 0.2$,²¹ the value being in accordance with calculated values for the ratio $n_{[\text{bound } 3]}/n_{[\text{polynucleotide}]}$ from the spectrophotometric titrations. This finding does not support the bis-intercalative binding mode, and it is in line with the next neighbour exclusion principle.¹⁸

**Fig. 3** Nonlinear dependence of ratio r (molar ratio of **3**–nucleic acid phosphates) and respective ΔT_m values found for ct-DNA at pH = 5.

The ΔT_m values obtained at pH = 5 and at pH = 7 are significantly different (Table 5). At pH = 5 stabilisation of ct-DNA is 5 times stronger than at pH = 7, while for poly A–poly U the difference is only by 50%. Observed results point to the strong ct-DNA over poly A–poly U preferential stabilisation of **3**

Table 6 ΔT_m values ($^{\circ}\text{C}$) of **3** in high ionic strength buffer pH = 5.0^{a,b}

	r		
	0.1	0.2	0.3
ct-DNA	2.0	3.0	4.0
poly A–poly U	23/0	29/0	3.1/0

^a See footnotes to Table 5. ^b T_m values of free polynucleotides: ct-DNA/77.2 $^{\circ}\text{C}$; poly A–poly U/48.0; 73.5 $^{\circ}\text{C}$, about biphasic transition see footnote ^c to Table 5.

at pH = 5, a feature not present at neutral pH. It is interesting to note that stabilisation of poly dA–poly dT is virtually the same at both pH values used, thus strong poly A–poly U over poly dA–poly dT preferential stabilisation of **3** observed at pH = 5, is actually reversed at pH = 7. Since not only basepair composition but also secondary structures of studied ds-polynucleotides are significantly different (B-helix of ct-DNA, A-helix of poly A–poly U and peculiar twisted helix with deep and narrow minor groove of poly dA–poly dT^{22,23}) it was not possible to distinguish features responsible for obtained selective thermal stabilisation between polynucleotides at same pH, as well as between different thermal stabilisations of same polynucleotide at pH = 5 and pH = 7, respectively.

To shed more light on the influence of electrostatic interactions on the thermal stabilisation of double helices in the presence of **3**, we have performed thermal melting experiments (at pH = 5) also at increased ionic strength with 0.1 mol dm^{-3} NaCl in respective buffer (Table 6). At pH = 5 ct-DNA–poly A–poly U preference at higher ionic strength is significantly lower, revealing much more pronounced inhibitive effect of added NaCl on thermal stabilisation of ct-DNA than of poly A–poly U. These two polynucleotides significantly differ in secondary structure, the former characterised by a much narrower and more hydrophobic minor groove compared to the shallow and wide minor groove of the latter.²⁰ Since the hydrophobicity of the poly dA–poly dT minor groove is even more pronounced than that of ct-DNA, it seems that minor groove properties are important for selectivity of polynucleotide thermal stabilisation induced by addition of **3**.

It is interesting to note that classical intercalators like ethidium bromide (**EB**) do not significantly change DNA/RNA preference stabilisation with the change of ionic strength (Table 7).²⁶

Also, at pH = 5 and pH = 7 the stabilisation effects of **EB** toward different polynucleotides are similar (Table 7). These observations point toward a strong impact of the pH (and consequently the number of positive charges of **3**) on the thermal stabilisation of ds-polynucleotides, thus electrostatic interactions of the non-intercalated part of **3** with negatively charged phosphates of polynucleotide playing also an important role in cumulative stabilisation of the polynucleotide double helix.

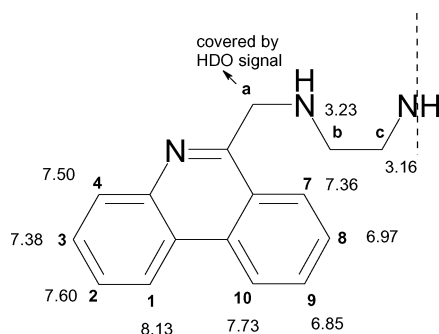
All the afore mentioned put forward the significance of the fine interplay between hydrophobic properties of the minor groove of

Table 7 Previously published²⁵ ΔT_m values ($^{\circ}\text{C}$) of **EB** in low and high ionic strength buffers pH = 5.0 and pH = 7.0

pH		$r = 0.3$	
		$I = 0.025 \text{ mol dm}^{-3}$	$I = 0.125 \text{ mol dm}^{-3}$
5	ct-DNA	17.3	3.2
	Poly dA–poly dT	14.0	3.0
	Poly A–poly U	36.1	10.7
7	ct-DNA	—	—
	Poly dA–poly dT	13.5	—
	Poly A–poly U	29.1	—

ds-polynucleotide and electrostatic interactions of the positively charged non-intercalated part of **3** and the negatively charged phosphates on thermal stabilisation of polynucleotides, resulting in observed selectivity.

¹H NMR experiments. All ¹H NMR experiments were performed in buffered D₂O solution (sodium cacodylate buffer, pD = 5.4, $\delta_{\text{OH}}(2 \text{ CH}_3) = 1.64 \text{ ppm}$, $I = 0.05 \text{ mol dm}^{-3}$) of **3** and all proton signals were assigned by 1D and 2D NMR analysis (Scheme 2).



Scheme 2 Chemical shifts (δ/ppm) of **3** ¹H NMR signals at $c = 1 \times 10^{-4} \text{ mol dm}^{-3}$ (Na cacodylate buffer, pD = 5.4, reference $\delta_{\text{OH}}(2 \text{ CH}_3) = 1.64 \text{ ppm}$, $I = 0.05 \text{ mol dm}^{-3}$).

The proton signals of **3** did not shift significantly in the concentration range $c(\mathbf{3}) = 2 \times 10^{-4} - 2 \times 10^{-3} \text{ mol dm}^{-3}$ indicating that there are no significant intermolecular interactions. ¹H NMR titrations with ct-DNA were done at $c(\mathbf{3}) = 2 \times 10^{-4} \text{ mol dm}^{-3}$ by successive additions of aliquots of DNA solution to cover the range of ratios $r_{[\mathbf{3}]/[\text{ct-DNA}]} = 2.5-0.1$. The height of proton signals attributed to CH₂ groups of the aliphatic linker of **3** did not change significantly upon adding ct-DNA, only a slight downfield shift of the proton signal attributed to the centrally positioned CH₂ groups in the linker was observed. Upon successive additions of ct-DNA, a substantial height decrease and broadening of ¹H NMR aromatic signals of **3** was observed, until they completely disappeared at $r = 0.25$. It is noteworthy that this value of ratio r is in good agreement with values of ratio n obtained by processing titration data with the Scatchard equation (Table 4) as well as with those estimated from thermal denaturation experiments (Fig. 3). Disappearance of aromatic proton signals of **3** strongly suggest intensive involvement of phenanthridine units into aromatic stacking interactions with ct-DNA.^{24,25} The rather low values of K_s and high n ratio values obtained for **3** (Table 4) as well as the ΔT_m values (Table 5) do not agree with a bis-intercalative binding mode of **3** to ct-DNA, but the complete disappearance of aromatic proton signals points to the equivalent involvement of both phenanthridinium units in intercalative binding mode. In all probability, aromatic units of **3** successively intercalate and dissociate from DNA, as it was proposed for its close analogues and termed “creeping” over ds-polynucleotide.³

Interactions of **3** with single stranded (ss-) polynucleotides

UV/Vis titrations. Addition of ss-polynucleotides at pH = 5 caused small hypochromic effects in the UV/Vis spectrum of **3** under conditions of excess of **3** over intercalation binding sites. Further additions of polynucleotides resulted in a substantial absorption increase of the sample due to the significant overlapping of UV/Vis spectra of **3** and ss-polynucleotides in excess. However, clear non-additivity of polynucleotide and **3** UV/Vis spectrum could be observed. Unfortunately, the limitations of the method prevented us from collecting enough titration data for accurate calculation of binding constants. At pH = 7

Table 8 Binding constants (K_s) and ratios n^a ([bound **3**]/[polynucleotide]) calculated from fluorimetric titrations of **3** ($c = 5 \times 10^{-6} \text{ mol dm}^{-3}$) with ss-polynucleotides at pH = 5 (buffer citric acid, $I = 0.03 \text{ mol dm}^{-3}$) and pH = 7 (buffer sodium cacodylate, $I = 0.05 \text{ mol dm}^{-3}$)

pH		n	$\log K_s$	I/I_0
5	poly A	0.2	5.0	2.50
	poly G	0.2	6.13	0.66
	poly C	0.2	5.43	1.68
	poly U	0.2	4.5	2.02
7	poly A	0.2	4.57	0.32
	poly G	0.2	5.12	0.25
	poly C	0.2	4.49	0.70
	poly U	0.2	4.37	0.75

^a For easier comparison of $\log K_s$ values the Scatchard equation was modified by fixing value of ratio $n = 0.2$.

addition of any polynucleotide to solution of **3** yielded instant precipitation.

Fluorimetric titrations. Since **3** exhibits strong fluorescence emission, it was possible to perform fluorimetric titrations with ss-polynucleotides. Excitation of **3** at $\lambda_{\text{max}} = 332 \text{ nm}$ was used for fluorimetric titrations for the same reasons as described in the above section on interactions with ds-polynucleotides. Processing of titration data by means of a modified Scatchard equation gave the binding constants listed in Table 8.

Among all ss-polynucleotides only the affinity of **3** towards poly U does not depend on pH. This observation could be attributed to the fact that poly U is the only ss-polynucleotide without a significantly organised secondary structure and protonation sites at the used pH's,²⁰ so its properties remain basically unchanged within the used pH range. It is obvious that a different number of positive charges of **3** does not significantly influence the overall stability of the **3**-poly U complex. All the above-mentioned suggests a dominant role of aromatic stacking interactions between phenanthridines of **3** and uracils of the polynucleotide in complex stability. The binding constants for **3**-poly U complexes are more than one order of magnitude higher than the respective K_s values observed for most classical intercalators (phenanthridinium and acridinium cations, $\log K_s < 3$),^{26,27} what strongly supports simultaneous and additive interactions of both phenanthridine units of **3** in binding to poly U.

The higher affinity of **3** towards poly A and poly C at pH = 5 could be the consequence of binding to double stranded structures (poly AH⁺-poly AH⁺ and poly CH⁺-poly CH⁺),²⁰ while at pH = 7 binding of **3** to the corresponding ss-polynucleotides resulted in lower affinity. The K_s values at pH = 5 are in agreement with this assumption, being of the same order of magnitude as those obtained for binding of **3** to ds-polynucleotides (Table 4). The double positive charge of **3** at pH = 5 compared to pH = 7 will also contribute to significantly higher binding constants under acidic conditions compared to those at neutral conditions.

The higher affinity of **3** towards poly G at both pH's than to other studied ss-polynucleotides reveals a significant role of additional stabilizing interactions specific for the **3**-poly G complex. Specific structural features of poly G compared to other ss-polynucleotides could play a significant role.²⁸ The observed specific spectroscopic effect upon addition of poly G to **3** (fluorescence quenching at pH = 5) could be attributed to the electron donating properties of guanine.^{29,30} Similar effects have been observed with proflavine²⁹ and 4,9-diazapyrene²⁶ derivative (increase of fluorescence for all nucleobases, quenching exclusively for guanine derivatives). An order of magnitude lower binding of **3**-poly G complex at pH = 7 than at pH = 5 again suggests a significant influence of the number of positive charges of **3**.

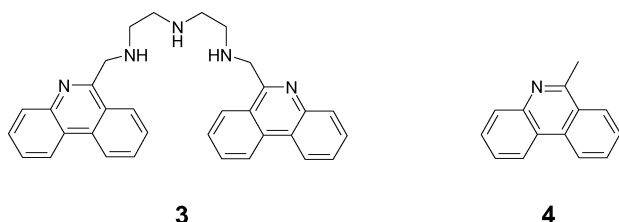


Fig. 4 Structures of studied compounds, **3** and its “monomer” **4**.

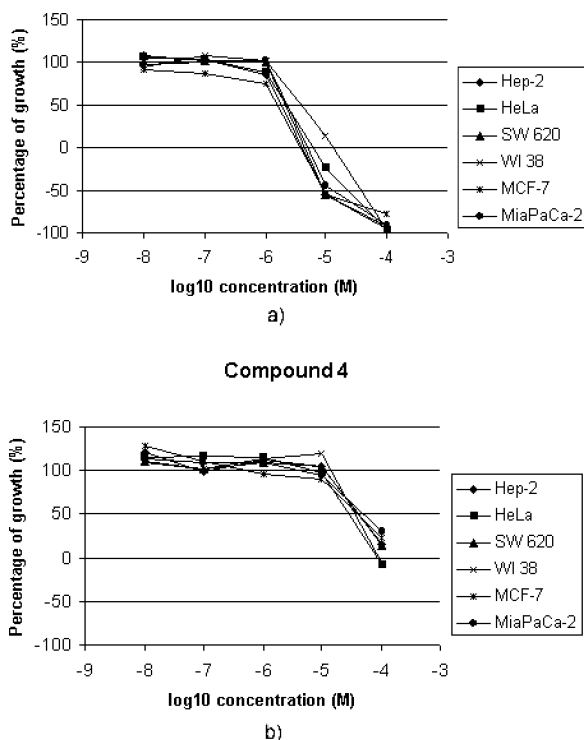


Fig. 5 Dose–response profiles for compounds **3** and **4** tested on various human cell lines *in vitro*. The cells were treated with compounds **3** and **4** at different concentrations, and the percentage of growth was calculated. Each point represents a mean value of four parallel samples in three individual experiments.

Antitumor activity assays

Among many antitumor drugs numerous are DNA intercalators¹ and some bis-intercalators (like *e.g.* echinomycin).³¹

Therefore, it was of highest interest to study cytotoxic effects of **3** on different tumor and normal cell lines. In addition, monomer **4**³² (Fig. 4) was studied for comparative purposes. The results presented in Table 9 and Fig. 5a clearly show a distinct antiproliferative activity of **3** towards five tumor cell lines (with IC_{50} in micromolar range). However, a slightly less pronounced inhibition of the growth of normal fibroblasts (WI 38) does not indicate selectivity towards tumor cells. Moreover, results presented in Table 9 indicate that the activity of **3** is more than one order of magnitude higher than observed for **4**. If the intercalation of the phenanthridine moiety would be the

sole mode of action, one would expect just double the activity for **3** as compared to **4**. This finding clearly demonstrates not only additive but also a positively cooperative effect of two phenanthridines and triamine linker assembled in the same molecule, which is also in accord with the results obtained for many bis-intercalative antitumor agents.³

Conclusions

The protonation state of **3** is strongly pH-dependent, **3** bearing four positive charges at pH = 5 and less than two at pH = 7. This is clearly reflected in the stability of **3**–nucleotide complexes: at pH = 5 binding constants (K_s) are proportional to the number of nucleotide phosphates, while at pH = 7 this is not the case.

Pronounced thermal stabilisation of double helices of ds-polynucleotides upon addition of **3**, hypochromic and bathochromic effects induced in UV/Vis spectrum of **3** upon addition of all studied polynucleotides and specific changes in ¹H NMR aromatic signals of **3** upon titration with ct-DNA are characteristic for aromatic $\pi \cdots \pi$ stacking interactions between aromatic moieties of **3** and polynucleotides, all strongly supporting the intercalative binding mode.²⁵ Binding constants (K_s) obtained for ds-polynucleotides are more than one order of magnitude higher than those observed for ss-polynucleotides—this finding can easily be correlated with the significantly larger aromatic surface of basepairs compared to single nucleobases—also in line with aromatic stacking interactions. However, values of ratio $n > 0.1$ and values of K_s and ΔT_m mostly of the same order of magnitude as found for classical mono-intercalators do not agree with bis-intercalation of **3** but suggest intercalation of only one phenanthridine unit with additional interactions of the non-intercalated positively charged part of the molecule with polynucleotide. As a final conclusion, aside from intercalation as a dominant binding interaction of **3** with ds-polynucleotides, a fine interplay between hydrophobic properties of the minor groove of ds-polynucleotide and electrostatic interactions of positively charged (pH dependent) non-intercalated part of **3** with the negatively charged phosphates are resulting in selective binding of **3** to different ds-polynucleotides.

Stability of most of the most **3**–ss-polynucleotide complexes is also dependent on the number of positive charges of **3**. The only exception was the **3**–poly U complex, whose stability was essentially independent of pH, very likely due to the specific structural properties of poly U. However, **3** exhibited the highest affinity and specific fluorescence sensing of poly G at pH = 5, again very likely due to the specific structural properties of poly G and the guanine base itself. As a general conclusion regarding ss-polynucleotides, **3** is a highly sensitive ligand addressing specific polymer structure and nucleobase nature, being additionally regulated by pH.

The one order of magnitude higher cytotoxicity of **3** compared to its “monomer” **4** can only be explained by cooperative action of the two phenanthridine units and the charged triamine linker of **3**. Since it is known that the microenvironment within solid tumors is slightly more acidic than in normal tissues,³³ and that a weakly acidic drug with $pK_a = 6.0$ will be concentrated inside the cell at 2.4-fold the extracellular drug concentration (*i.e.* weakly

Table 9 *In vitro* inhibition of tumor- and normal human fibroblast (WI 38) cell growth

Compound	$IC_{50}/\mu\text{mol dm}^{-3a}$					
	Hep 2	HeLa	MiaPaCa-2	SW 620	MCF-7	WI 38
3	1.9 ± 0.3	2.5 ± 1.2	2.5 ± 1.2	2.0 ± 0.6	1.5 ± 0.4	4.2 ± 1.0
4	41.2 ± 7.3	29.7 ± 15.3	50.0 ± 7.6	38.6 ± 20.0	40.0 ± 23.6	36 ± 1.7

^a IC_{50} is the concentration that causes a 50% cell growth reduction.

acidic drugs are well-suited for treatment of tumors with large acidic regions⁹ the demonstrated pH dependent properties of **3** make it a promising candidate for further *in vivo* testing.

Experimental

Spectroscopy

¹H-NMR spectra were recorded on Bruker spectrometers at 300 and 600 MHz. Chemical shifts (δ) in ¹H NMR spectra are expressed in ppm and *J* values in Hz. All NMR measurements were done in buffered D₂O solution (Na cacodylate buffer, pD = 5.4, *I* = 0.05 mol dm⁻³), using buffer proton signal ($\delta_{\text{OH}}(2 \text{ CH}_3) = 1.64$ ppm) as reference. Signal multiplicities are denoted as s (singlet), d (doublet), t (triplet), q (quartet) and m (multiplet). Electronic absorption spectra were obtained on Varian Cary 100 Bio spectrometer and fluorescence spectra were recorded on a Varian Cary Eclipse fluorimeter, both in quartz cuvettes (1 cm). ESI MS spectra were obtained using Waters Micromass ZQ. All measurements were performed in aqueous buffered solutions at pH = 5 (Na citrate buffer, *I* = 0.027 mol dm⁻³ or Na cacodylate buffer; *I* = 0.05 mol dm⁻³) and at pH = 7 (Na cacodylate buffer; *I* = 0.05 mol dm⁻³). Polynucleotides were purchased as noted: poly G–poly C, poly A–poly U, poly dA–poly dT, poly A, poly G, poly C, poly U (Sigma), calf thymus ct-DNA (Aldrich). Polynucleotides were dissolved in Na-cacodylate buffer, *I* = 0.05 mol dm⁻³, pH = 7. Calf thymus ct-DNA was additionally sonicated and filtered through a 0.45 μm filter.^{34,35} Polynucleotide concentration was determined spectroscopically,³⁵ and expressed as concentration of backbone phosphates. Spectroscopic titrations were performed by adding portions of polynucleotide solution into the solution of the studied compound.

Absorbance and fluorescence emission of **3** was proportional to its concentration under the experimental conditions. Titration data were corrected for dilution. Excitation of **3** at $\lambda_{\text{max}} = 332$ nm was used for fluorimetric titrations since nucleotides and polynucleotides do not absorb light at $\lambda > 300$ nm and at $\lambda > 340$ nm excitation and emission spectra of **3** significantly overlap. Binding constants (K_s) for **3**–nucleotide complexes were calculated by SPECFIT program¹² from fluorimetric titration data. Processing of titration data by means of the Scatchard equation was used for the calculation of ratio *n* ([bound **3**]/[polynucleotide]) and binding constants (K_s) for **3**–polynucleotide complexes.¹⁷ Values for K_s and *n* given in Tables 4 and 8 all have satisfactory correlation coefficients (>0.999). Thermal melting curves for DNA, RNA and their complexes with **3** were determined as previously described³³ by following the absorption change at 260 nm as a function of temperature. Absorbance of **3** was subtracted from every curve, and the absorbance scale was normalized. T_m values are midpoints of the transition curves, determined as maximum of the first derivative plots and checked graphically by the tangent method.³³ ΔT_m values were calculated subtracting T_m of the free nucleic acid from T_m of the complex. Every ΔT_m value here reported was the average of at least two measurements; the error in ΔT_m is ± 0.5 °C.

Synthesis of 1,9-bis(6-phenanthridinium)-2,5,8-triazanonane tetrahydrochloride (**3**)

A solution of diethylenetriamine (32 μl ; 3 mmol, 1 equivalent) and phenanthridine-5-aldehyde (**1**, 136 mg; 0.66 mmol, 2.2 equivalents) in solvent mixture CH₃OH–CH₂Cl₂ = 1 : 1 (9 ml) under Ar was stirred in the dark at room temperature for 24 hours. The solution was then cooled to 0 °C and NaBH₄ (30 mg, 8 mmol, 2.6 equivalents) was added under dry conditions. Suspension was stirred at 0 °C for 1 hour and then at room temperature overnight. Solvents were evaporated at *T* < 30 °C, the oily residue suspended in water (10 ml) and extracted with three portions of 5 ml of CH₂Cl₂. The organic phase was

dried on Na₂SO₄ and solvent evaporated. Addition of 3.5 ml (app. 8 equivalents) of 0.7 mol dm⁻³ HCl–CH₃OH to the crude residue resulted in formation of a green precipitate, which after recrystallization from hot CH₃OH and successive washing with small portions of cold CH₃OH gave a creamy, white precipitate. ¹H NMR (for assignment see Scheme 2; δ_{H} /ppm, D₂O, pD = 5.4; buffered with sodium cacodylate buffer; *I* = 0.001 mol dm⁻³, *c*(**3**) = 1×10^{-4} mol dm⁻³, reference 2 CH₃ of the cacodylate, $\delta_{\text{OH}} = 1.64$ ppm): 3.16 (br; 4H; c-CH₂); 3.23 (br; 4H; b-CH₂); ≈ 4.8 (2H; a-CH₂); 6.85 (dd, 2H_{phen}-C9); 6.97 (dd, 2H-H_{phen}8); 7.36 (d, 2H-H_{phen}7); 7.38 (dd, 2H-H_{phen}3); 7.50 (d, 2H-H_{phen}4); 7.60 (dd, 2H-H_{phen}2); 7.73 (d, 2H-H_{phen}10); 8.13 (d, 2H-H_{phen}1). ESI-MS (*m/z*) 486.1 (**3** – H⁺); 243.7 (**3** – 2H⁺). Anal. Calcd for C₃₂H₃₁N₅ × 4 HCl (Mr = 631.45): C 60.87, H 5.59, N 11.09%; Found: C 60.43, H 5.87, N 11.39%.

Antitumor activity assays

HeLa (cervical carcinoma), MCF-7 (breast carcinoma), SW 620 (colon carcinoma), MiaPaCa-2 (pancreatic carcinoma), Hep-2 (laryngeal carcinoma) and WI 38 (diploid fibroblasts) cells were cultured as monolayers and maintained in Dulbecco's modified Eagle's medium (DMEM) supplemented with 10% fetal bovine serum (FBS), 2 mmol dm⁻³ L-glutamine, 100 U ml⁻¹ penicillin and 100 μg ml⁻¹ streptomycin in a humidified atmosphere with 5% CO₂ at 37 °C. Growth inhibition activity was assessed according to the slightly modified procedure performed at the National Cancer Institute, Developmental Therapeutics Program.^{36,37} Cells were inoculated onto standard 96-well microtiter plates on day 0. Cell concentrations were adjusted according to the cell population doubling time (PDT): 1×10^4 ml⁻¹ for HeLa, Hep-2, MiaPaCa-2 and SW 620 cell lines (PDT = 20–24 hours) 2×10^4 ml⁻¹ for MCF-7 cell lines (PDT = 33 hours) and 3×10^4 ml⁻¹ for WI 38 (PDT = 47 hours). Test agents were then added in five 10-fold dilutions (10^{-8} to 10^{-4} mol dm⁻³) and incubated for further 72 hours. Working dilutions were freshly prepared on the day of testing. Solvent (0,001 mol dm⁻³ HCl) was also tested for possible inhibitory activity by adjusting its concentration to be the same as in working concentrations. After 72 hours of incubation, cell growth rate was evaluated by performing MTT assay,³⁸ which detects dehydrogenase activity in viable cells. Absorbance (OD, optical density) was measured in a microplate reader at 570 nm. Percentage of growth (PG) of the cell lines was calculated according to one or the other of the following two expressions:

If (mean OD_{test} – mean OD_{tzero}) ≥ 0 then
$$\text{PG} = 100 \times (\text{mean OD}_{\text{test}} - \text{mean OD}_{\text{tzero}}) / (\text{mean OD}_{\text{ctrl}} - \text{mean OD}_{\text{tzero}}).$$

If (mean OD_{test} – mean OD_{tzero}) < 0 then
$$\text{PG} = 100 \times (\text{mean OD}_{\text{test}} - \text{mean OD}_{\text{tzero}}) / \text{OD}_{\text{tzero}}.$$

Where:

Mean OD_{tzero} = average optical density before exposure of cells to the test compound.

Mean OD_{test} = average optical density after the desired period of time.

Mean OD_{ctrl} = average optical density after the desired period of time with no exposure of cells to the test compound.

Each test point was performed in quadruplicate in three individual experiments. Results are expressed as IC₅₀, which is the concentration necessary for 50% inhibition. IC₅₀ values for each compound are calculated from dose–response curves using linear regression analysis by fitting the test concentrations that give PG values above and below the reference value (*i.e.* 50%). Each result is a mean value of three separate experiments.

References

- 1 M. Demeunynck, C. Bailly and W. D. Wilson, *DNA and RNA binders*, Wiley-VCH, Weinheim, 2002.
- 2 E. J. Fechter, B. Olenyuk and P. B. Dervan, *Angew. Chem., Int. Ed.*, 2004, **43**, 3591–3594.

- 3 L. P. G. Wakelin, *Med. Res. Rev.*, 1986, **6**(3), 315–335.
- 4 K. D. Copeland, M. P. Fitzsimons, R. P. Houser and J. K. Barton, *Biochemistry*, 2002, **41**, 343–356.
- 5 F. Pina, M. A. Bernardo and E. García-España, *Eur. J. Inorg. Chem.*, 2000, **10**, 2143–2157.
- 6 J. Barbet, B. P. Roques, S. Combrisson and J. B. LePecq, *Biochemistry*, 1976, **15**, 2642–2650; O. Baudoin, F. Gonnet, M.-P. Teulade-Fichou, J.-P. Vigneron, J.-C. Tabet and J.-M. Lehn, *Chem. Eur. J.*, 1999, **5**, 2762–2771; N. Berthet, J. Michon, J. Lhomme, M.-P. Teulade-Fichou, J.-P. Vigneron and J.-M. Lehn, *Chem. Eur. J.*, 1999, **5**, 3625–3629; M. Jourdan, J. Garcia, J. Lhomme, M.-P. Teulade-Fichou, J.-P. Vigneron and J.-M. Lehn, *Biochemistry*, 1999, **38**, 14205–14213; A. Slama-Schwok, M.-P. Teulade-Fichou, J.-P. Vigneron, E. Taillandier and J.-M. Lehn, *J. Am. Chem. Soc.*, 1995, **117**, 6822–6831.
- 7 M. T. Albelda, M. A. Bernardo, P. Díaz, E. García-España, J. S. de Melo, F. Pina, C. Soriano and S. V. Luis, *Chem. Commun.*, 2001, 1520–1521.
- 8 M. M. Becker and P. B. Dervan, *J. Am. Chem. Soc.*, 1979, **101**, 3664–3666.
- 9 N. Raghunand and R. J. Gillies, *Drug Resist. Updates*, 2000, **3**, 39–47.
- 10 T. Eicher and A. Kruse, *Synthesis*, 1985, 612.
- 11 L.-M. Tumir, I. Piantanida, P. Novak and M. Žinić, *J. Phys. Org. Chem.*, 2002, **15**, 599–607.
- 12 Specfit Global Analysis, a Program for Fitting, Equilibrium and Kinetic Systems, Using Factor Analysis & Marquardt Minimization H. Gampp, M. Maeder, C. J. Meyer and A. D. Zuberbuehler, *Talanta*, 1985, **32**, 257–264; M. Maeder and A. D. Zuberbuehler, *Anal. Chem.*, 1990, **62**, 2220–2224.
- 13 P. Čudić, M. Žinić, V. Tomišić, V. Simeon, J.-P. Vigneron and J.-M. Lehn, *J. Chem. Soc., Chem. Commun.*, 1995, 1073–1075.
- 14 A. Odani, H. Masuda, O. Yamauchi and S. Ishiguro, *Inorg. Chem.*, 1991, **30**, 4486–4488.
- 15 I. Piantanida, V. Tomišić and M. Žinić, *J. Chem. Soc., Perkin Trans. 2*, 2000, 375–383.
- 16 L.-M. Tumir, I. Piantanida, I. Juranović Cindrić, T. Hrenar, Z. Meić and M. Žinić, *J. Phys. Org. Chem.*, 2003, **16**, 891–899.
- 17 G. Scatchard, *Ann. N.Y. Acad. Sci.*, 1949, **51**, 660–672; J. D. McGhee and P. H. von Hippel, *J. Mol. Biol.*, 1976, **103**, 679–684.
- 18 H. W. Zimmermann, *Angew. Chem., Int. Ed. Engl.*, 1986, **25**, 115–196.
- 19 M. Cory, D. D. McKee, J. Kagan, D. W. Henry and J. A. Miller, *J. Am. Chem. Soc.*, 1985, **107**, 2528–2536.
- 20 C. R. Cantor and P. R. Schimmel, *Biophysical Chemistry*, WH Freeman and Co., San Francisco, 1980, vol. 3, pp. 1109–1181.
- 21 W. D. Wilson, F. A. Tanious, M. Fernandez-Saiz and C. T. Rigl, *Evaluation of Drug/Nucleic Acid Interactions by Thermal Melting Curves*, from: *Methods in Molecular Biology*, vol. 90, *Drug-DNA Interaction Protocols*, ed. K. R. Fox, Humana Press Inc., Totowa, N.Y., 1998.
- 22 H. C. M. Nelson, J. T. Finch, B. F. Luisi and A. Klug, *Nature*, 1987, **330**, 221–226.
- 23 W. D. Wilson, Y.-H. Wang, C. R. Krishnamoorthy and J. C. Smith, *Biochemistry*, 1985, **24**, 3991–3999.
- 24 J. Sartorius and H.-J. Schneider, *FEBS Lett.*, 1995, **374**, 387–392.
- 25 G. Dougherty and J. R. Pilbrow, *Int. J. Biochem.*, 1984, **16**, 1179–1192; E. C. Long and J. K. Barton, *Acc. Chem. Res.*, 1990, **23**, 273–279.
- 26 I. Piantanida, B. S. Palm, M. Žinić and H.-J. Schneider, *J. Chem. Soc., Perkin Trans. 2*, 2001, 1808–1816.
- 27 J. Kapuscinski and Z. Darzynkiewicz, *J. Biomol. Struct. Dyn.*, 1987, **5**, 127–143.
- 28 W. Saenger, *Principles of Nucleic Acid Structure*, Springer, New York, 1988, ch. 13.6, pp. 315–320; J. T. Davis, *Angew. Chem.*, 2004, **43**, 668–698.
- 29 S. Georghiou, *Photochem. Photobiol.*, 1977, **26**, 59.
- 30 J. Ramstein and M. Leng, *Biochim. Biophys. Acta*, 1972, **281**, 18.
- 31 X. Gao and D. J. Patel, *Biochemistry*, 1988, **27**, 1744–1751.
- 32 Monomer **4** is actually the starting material for the synthesis of **1**, and was prepared according to previously described procedures (see Experimental).
- 33 P. Wong, C. Lee and I. F. Tannock, *Clin. Cancer Res.*, 2005, **11**, 3553–3557.
- 34 J. B. Chaires, N. Dattagupta and D. M. Crothers, *Biochemistry*, 1982, **21**, 3933–3940.
- 35 B. S. Palm, I. Piantanida, M. Žinić and H.-J. Schneider, *J. Chem. Soc., Perkin Trans. 2*, 2000, 385–392.
- 36 M. R. Boyd and K. D. Paull, *Drug Dev. Res.*, 1995, **34**, 91–109.
- 37 I. Jarak, M. Kralj, L. Šuman, G. Pavlović, J. Dogan, I. Piantanida, M. Žinić, K. Pavelić and G. Karminski-Zamola, *J. Med. Chem.*, 2005, **48**, 2346–2360.
- 38 T. Mossman, *J. Immunol. Methods*, 1983, **65**, 55–61.